

# Material Characterization of $(\text{Bi}_{1/2}\text{Na}_{1/2})_{0.94}\text{Ba}_{0.06}\text{TiO}_3$ Ceramic as a Lamb Wave Device Substrate

Napadon Kaewkamnerd, Tadashi Takenaka, Koichiro Sakata and Kohji Toda<sup>1</sup>

Faculty of Science and Technology, Science University of Tokyo,  
Noda, Chiba 278, Japan

<sup>1</sup>Department of Electronic Engineering, National Defense Academy,  
Hashirimizu, Yokosuka 239, Japan

(Received October 13, 1995; accepted June 21, 1996)

**Key words:** piezoelectric ceramic, material constant, Lamb wave device, Lamb wave propagation

A lead-free piezoelectric ceramic  $(\text{Bi}_{1/2}\text{Na}_{1/2})_{0.94}\text{Ba}_{0.06}\text{TiO}_3$  (BNBT-6) is evaluated for possible use as a new substrate material for Lamb wave devices, with consideration of the effect of manganese carbonate ( $\text{MnCO}_3$ ) as a dopant. Lamb wave phase velocities and the electromechanical coupling constant of an interdigital transducer on the piezoelectric ceramic plate are represented as a function of the product of frequency and substrate thickness. The numerical analysis results of the Lamb wave phase velocities are in good agreement with the results obtained from the measurement of the center frequencies of prepared Lamb wave devices. The analyzed propagation characteristics show that the BNBT-6+Mn0.5 (wt%) ceramics are useful in constructing a Lamb wave device with high mechanical strength.

## 1. Introduction

Electromechanical functional parts have assumed importance in electronics toward the realization of higher functions. The Rayleigh wave (SAW) propagating in a semiinfinite elastic medium is one boundary surface characterized by energy localization near the boundary surface of the elastic medium. The Lamb wave has different characteristics from the Rayleigh wave in that it propagates in a thin elastic substrate with boundary surfaces.<sup>(1)</sup> The Lamb wave possesses a large velocity dispersion with the capability of using two surfaces and has the possibility of possessing an electromechanical coupling constant ( $k^2$ )

larger than that possessed by the Rayleigh wave employing the same substrate material.<sup>(2-4)</sup> By putting these features into practical use, we can fabricate unique devices. An interdigital transducer (IDT) excites and detects a surface acoustic wave (SAW) effectively on a piezoelectric substrate. The IDT can also be used as a Lamb wave transducer. A Lamb wave excited by the IDT carries energy from the input to the output of the acoustic device.<sup>(5)</sup>

Typical piezoelectric ceramics for use as substrate materials in elastic wave applications are  $\text{Pb}(\text{Zr},\text{Ti})\text{O}_3$  (PZT) or PZT-based multicomponent systems with a rhombohedral ( $F_\alpha$ )-tetragonal ( $F_\beta$ ) morphotropic phase boundary (MPB) composition, and perovskite-type  $\text{PbTiO}_3$  (Pt)-based or  $\text{PbZrO}_3$  (PZ)-based materials. Another type of piezoelectric ceramic is lead-free or low-lead-content materials obtained by the suppression of PbO evaporation during the sintering process.

Bismuth sodium titanate,  $\text{Bi}_{1/2}\text{Na}_{1/2}\text{TiO}_3$  (BNT), is strongly ferroelectric and expected to be a lead-free candidate material for piezoelectric applications.<sup>(6-10)</sup> However, its difficult poling process must be overcome for practical application of the material. Recently, a solid solution of BNT with a tetragonal perovskite structure has been shown to be useful because of its superior properties arising from the rhombohedral-tetragonal morphotropic phase boundary (MPB) and because its difficult poling process has been overcome.<sup>(11)</sup> In this work,  $(\text{Bi}_{1/2}\text{Na}_{1/2})_{0.94}\text{Ba}_{0.06}\text{TiO}_3$  (BNBT-6), which is a BNT-based solid solution around a MPB, is studied for possible use as a new type of elastic wave device substrate. Propagation characteristics of Lamb waves on the BNBT-6 piezoelectric ceramic plates are represented on the phase velocity and electromechanical coupling constant.

## 2. Sample Preparation and Evaluation of Material Constants

BNBT ceramic samples were prepared through a conventional sintering method. The starting raw materials were reagent-grade metal oxide or carbonate powders of  $\text{Bi}_2\text{O}_3$ ,  $\text{NaCO}_3$ ,  $\text{BaCO}_3$ ,  $\text{TiO}_2$  with 99%(+) purity. The mixed powders, after calcining at  $800^\circ\text{C}$  for one hour, were sintered at  $1200^\circ\text{C}$  for two hours in air. BNBT-6+ $\text{MnCO}_3$  (x wt%) ceramic samples were also prepared using the above procedure. Poling treatments were carried out at  $40^\circ\text{C}$  in a stirred silicone oil bath by applying a dc electric field of 3 kV/mm for 5 minutes, in the thickness direction.

Figure 1 shows the mechanical quality factor  $Q_m$  corresponding to the radial mode of a prepared ceramic disk as a function of the dopant concentration (Mn). The peak value of  $Q_m$  occurs at a dopant concentration of 0.5 wt%. Temperature dependences of the dielectric constant,  $\epsilon_s$ , and loss tangent,  $\tan \delta$ , are shown in Fig. 2 for the BNBT-6 ceramic sample and that containing 0.5 wt% Mn. The dielectric constant is smaller than those of conventional PZT or PZT-based ceramics. It is obvious that the presence of Mn in the BNBT-6 ceramic sample improves the dielectric properties. Weibull plots of the third point-bending strength and fracture probability,  $F(=1-S)$ , are shown in Fig. 3 for BNBT-6 and BNBT-6+Mn0.5 (wt%). BNBT-6 has a bending strength much larger than those of conventional piezoelectric ceramics. Material constants of the BNBT-6 and BNBT-

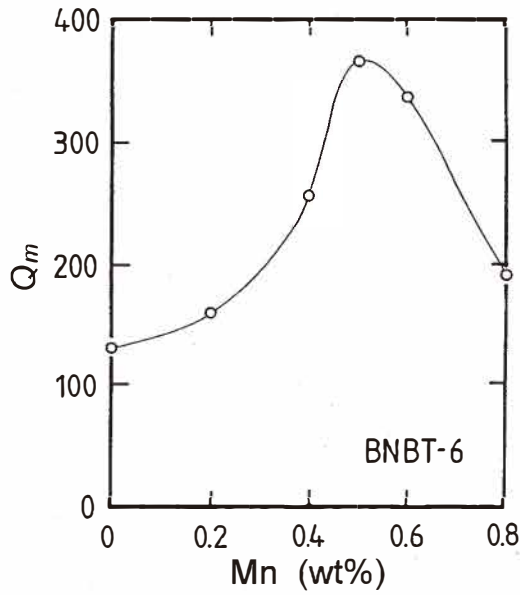


Fig. 1. Relationship between mechanical quality factor  $Q_m$  and Mn concentration.

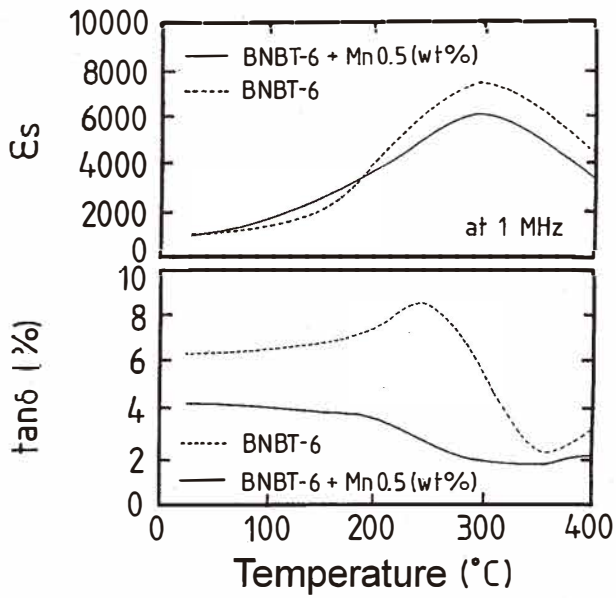


Fig. 2. Temperature dependences of dielectric constant  $\epsilon_s$  and loss tangent tan  $\delta$ .

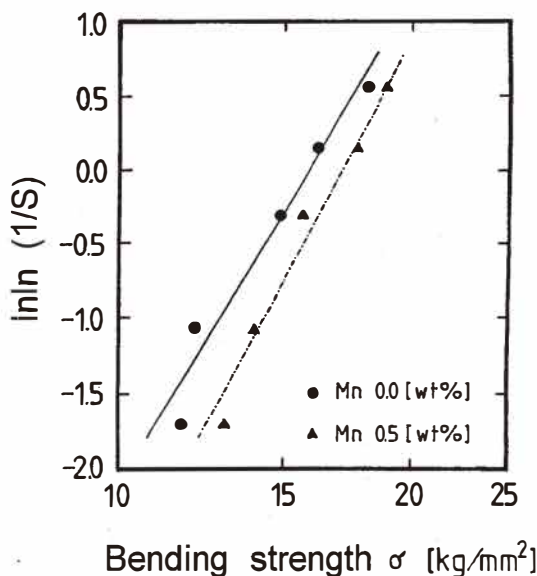


Fig. 3. Weibull plots obtained from relationship between bending stress and fracture probability  $F(=1-S)$ .

6+Mn0.5 (wt%) ceramics are listed in Table 1, obtained on the basis of IRE (IEEE) standards using an impedance analyzer (YHP 4192A).<sup>(12)</sup> The electromechanical coupling factor,  $K$ , was calculated from Onoe and Jyumonji's formula.<sup>(13)</sup> For the numerical analysis of Lamb wave propagation characteristics, elastic stiffness at constant electric field,  $C^E$ , piezoelectric coupling constant,  $e$ , and dielectric permittivity at constant strain,  $\epsilon_s$ , were calculated using the data shown in Table 1.

### 3. Lamb Wave Propagation Characteristics

Lamb waves propagate in a plate with finite thickness, depending on the plate thickness and the wavelength. The elastic plate waves are classified into two modes, symmetrical (S) and antisymmetrical (A), from the pattern of particle displacements. Lamb wave phase velocities are numerically calculated as a function of the product of frequency  $f$  and plate thickness  $d$ , and the results are shown in Figs. 4(a) and 4(b) for BNBT-6 and that containing 0.5 wt% Mn, respectively. The numerical analysis procedure is based on that described in refs. 14 and 15, under various electrical boundary conditions. The numerical results are compared with the experimental results from three kinds of Lamb wave devices with interdigital transducers (IDTs). The IDT with 10 finger pairs had three kinds of interdigital periodicities of 300, 500, and 800  $\mu\text{m}$ . The substrate was about 15 mm in diameter and 350

Table 1  
Material constants of the BNBT-6 ceramic and BNBT-6+Mn0.5 (wt%) ceramic.

Sample	BNBT-6	BNBT-6+Mn0.5 (wt%)
Coupling factor (%)		
$k_t$	52.9	49.80
$k_p$	30.2	28.90
$k_{31}$	19.2	18.24
$k_{33}$	55.0	53.60
$k_{15}$	49.8	48.80
Frequency constant (Hz·m)		
$N_t$	2535	2682
$N_p$	2997	3055
$N_{31}$	2264	2367
$N_{33}$	2506	2446
$N_{15}$	1586	1581
Dielectric constant		
$\epsilon_{11}^s/\epsilon_0$	1400	1200
$\epsilon_{33}^s/\epsilon_0$	580	524
Measured density (kg/m <sup>3</sup> )		
$\rho_0$	5680	5630
Elastic constant ( $\times 10^{10}$ (N/m <sup>2</sup> ))		
$c_{11}^E$	12.50	15.30
$c_{12}^E$	2.70	4.80
$c_{13}^E$	2.07	5.09
$c_{33}^E$	10.50	12.20
$c_{55}^E$	4.30	4.29
$c_{66}^E$	4.89	5.24
Piezoelectric constant (C/m <sup>2</sup> )		
$e_{24}$	11.50	10.40
$e_{31}$	-3.55	-1.03
$e_{33}$	11.50	10.80
Dielectric constant		
$\epsilon_{11}^s/\epsilon_0$	1050	914
$\epsilon_{33}^s/\epsilon_0$	405	373

$\mu\text{m}$  in thickness. The poling axis was in the thickness direction. The fingers of the IDTs were deposited on the free surface of the substrate via a mask with an electrode pattern which was about a  $0.3 \mu\text{m}$ -thick Al thin film. The measured data denoted by the open circles in Fig. 4 were obtained from the product of the center frequency and the interdigital periodicity. There is good agreement between the calculated and the measured data.

In using IDTs for generating and detecting Lamb waves, the electromechanical coupling constant  $k^2$  is an essential value.<sup>(16)</sup>  $k^2$  can be defined from the Lamb wave velocities on the electrically free (opened) and metallized (shorted) surfaces,  $V_o$  and  $V_s$ , by a relation  $k^2 = 2(V_o - V_s)/V_s$ . Figure 5 shows the calculated  $k^2$  dependence on  $fd$  for BNBT-6 and

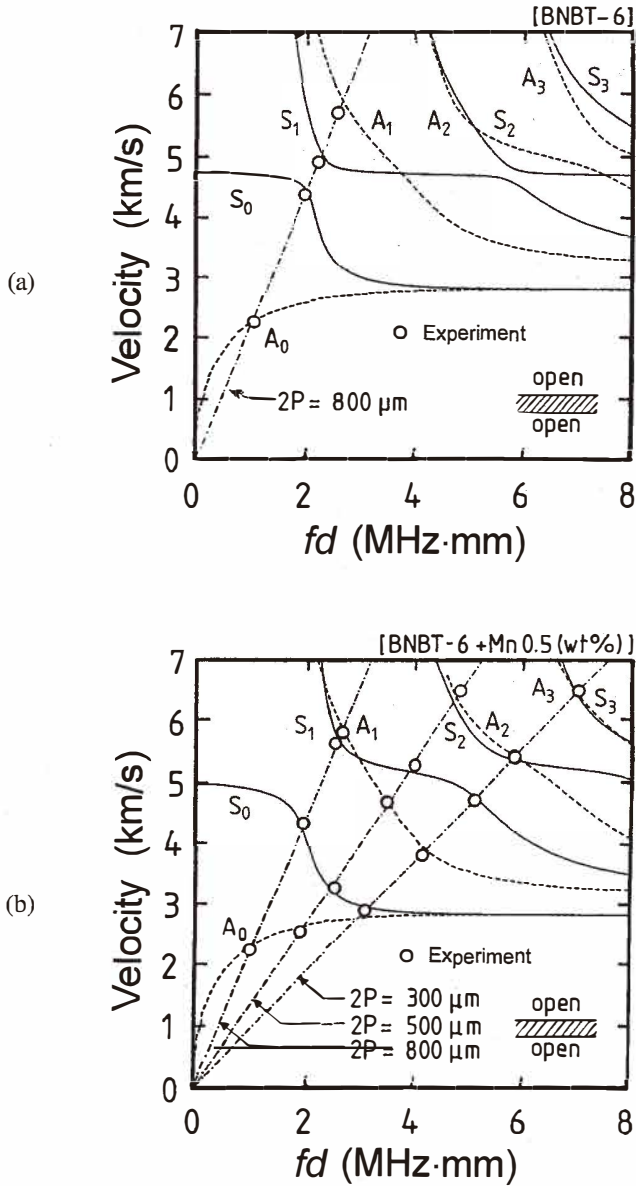


Fig. 4. Lamb wave velocities as a function of the product of frequency and plate thickness, for two kinds of substrate materials: (a) BNBt-6 and (b) BNBt-6+Mn0.5 (wt%).

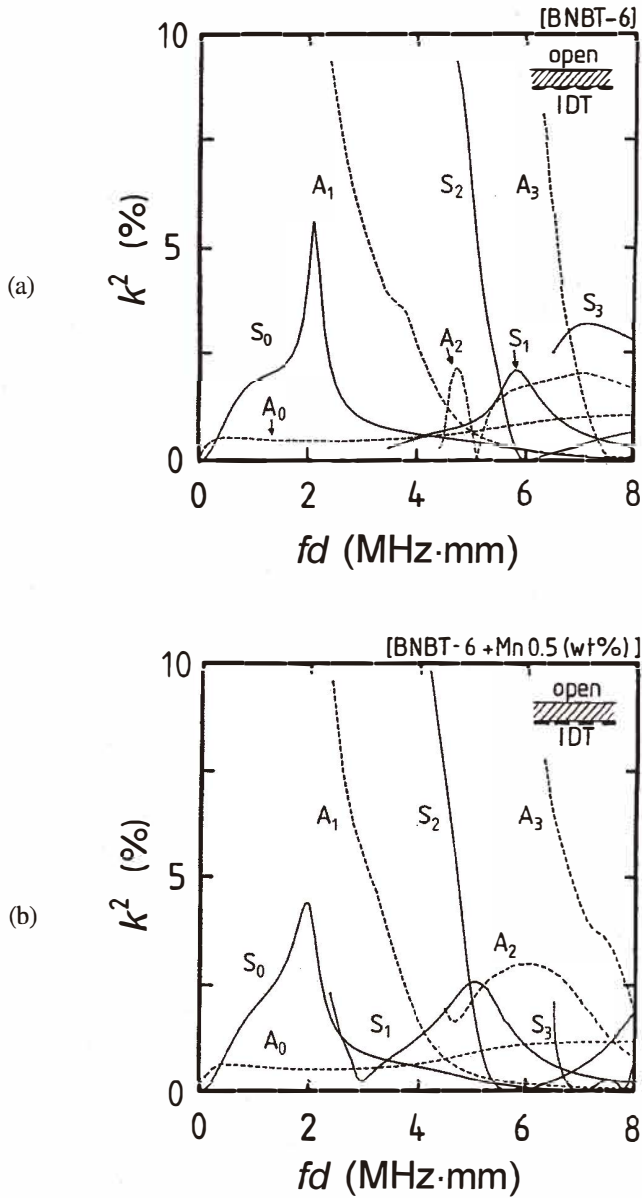


Fig. 5. Calculated  $k^2$  values as a function of the product of frequency and plate thickness, for two kinds of substrate materials: (a) BNBT-6 and (b) BNBT-6+Mn0.5 (wt%).

BNBT-6+0.5 wt% Mn. Experimental frequency dependences of insertion loss and phase delay of the Lamb wave device with an interdigital periodicity of  $800 \mu\text{m}$  on the BNBT-6+Mn0.5 (wt%) substrate are given in Fig. 6, and are consistent with the calculated results shown in Figs. 4 and 5. The  $k^2$  values of the zeroth-order symmetrical mode ( $S_0$ ), first-order antisymmetrical mode ( $A_1$ ) and  $S_2$  mode are useful for device fabrication in certain  $fd$  regions, compared with the  $k^2$  value of  $\text{LiNbO}_3$ , although the value for the Rayleigh mode is not large.

When a feedback loop is constructed via an amplifier between two IDTs of the Lamb wave device, a delay line oscillator is realized. A typical spectral response of a delay line oscillator using the  $A_1$  mode on the BNBT-6+Mn0.5 (wt%) ceramic plate is shown in Fig. 7. Thus, the oscillator can be used for practical operation in a single mode.

#### 4. Conclusions

Material constants of a lead-free piezoelectric ceramic,  $(\text{Bi}_{1/2}\text{Na}_{1/2})_{0.94}\text{Ba}_{0.06}\text{TiO}_3$ , have been evaluated. The Mn-doped BNBT-6 is characterized by improved dielectric property and high mechanical strength, while maintaining a high electromechanical coupling factor. Numerical analysis results of Lamb wave propagation characteristics have been compared with the experimental results, which suggest that the BNBT-6 can be used as a new type of lead-free piezoelectric substrate for Lamb wave devices.

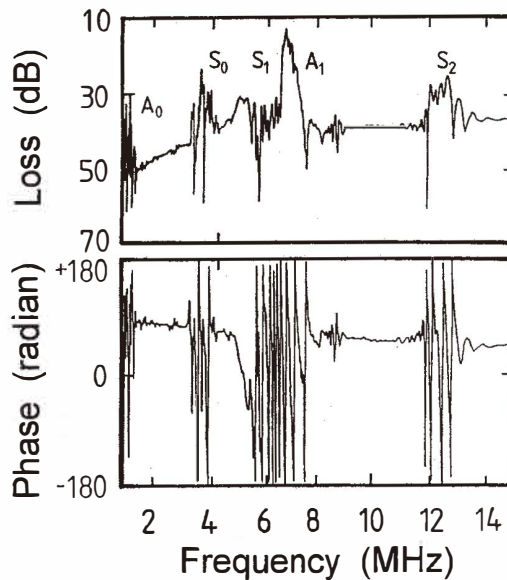


Fig. 6. Measured frequency dependences of insertion loss and phase delay of Lamb wave device mounted on BNBT-6+ Mn0.5 (wt%), where interdigital periodicity of IDT was  $800 \mu\text{m}$ .



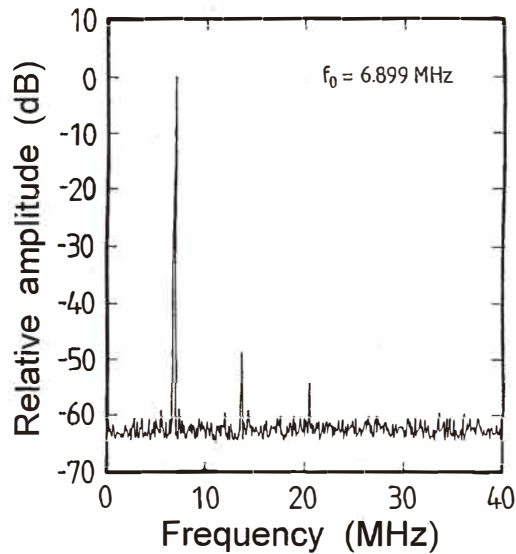


Fig. 7. Spectral response of delay line oscillator composed of Lamb wave device on BNB<sub>T</sub>-6+Mn0.5 (wt%) plate and amplifier.

### References

- 1 I. A. Victorov: Rayleigh and Lamb Waves (Plenum Press, New York, 1967) Ch. 2.
- 2 K. Toda: J. Appl. Phys. **44** (1973) 56.
- 3 K. Toda and K. Mizutani: J. Acoust. Soc. Am. **74** (1983) 677.
- 4 S. W. Wenzel and R. M. White: IEEE Trans. Electron Devices **ED-35** (1988) 735.
- 5 S. G. Joshi and Y. Jin: J. Appl. Phys. **70** (1991) 4113.
- 6 G. A. Smolensky, V. A. Isupov, A. I. Agranovskaya and N. N. Krainik: Soviet Physics-Solid State **2** (1961) 2651.
- 7 K. Sakata and Y. Masuda: Ferroelectrics **7** (1974) 347.
- 8 M. S. Hagiyevev, I. H. Ismailzade and A. K. Abiyev: Ferroelectrics **56** (1984) 215.
- 9 J. Suchanicz, K. Roleder, A. Kania and J. Handerek: Ferroelectrics **77** (1988) 107.
- 10 T. Takenaka and K. Sakata: Exhibits of "The Fourth U.S.-Japan Seminar on Dielectric and Piezoelectric Ceramics" (ONR, USA Dec. 1988) Vol. 1, p.146.
- 11 G. W. Farnell: "Acoustic Surface Waves", ed. A. A. Oliner (Springer-Verlag, Berlin, 1987) p. 13.
- 12 IRE Standards on Piezoelectric Crystals: Measurements of Piezoelectric Ceramics, 1961; IEEE Standard on Piezoelectricity, IEEE Std 176.
- 13 M. Onoe and H. Jyumonji: J. Acoust. Soc. Am. **41** (1967) 974.
- 14 J. J. Campbell and W. R. Jones: IEEE Trans. Sonics Ultrason. **SU-15** (1968) 209.
- 15 G. W. Farnell: IEEE Trans. Sonics Ultrason. **SU-17** (1970) 229.
- 16 K. Toda and K. Ibuki: Ferroele. **73** (1987) 419.